İSTANBUL UNIVERSITY CERRAHPAŞA

ORIGINAL ARTICLE
Electrica 2023; 23(2): 397-405

Detection of Damaged Structures From Satellite Imagery Processed by Autoencoder With Boruta Feature Selection Method

Nedim Muzoğlu[1], Ertuğrul Adıgüzel[2], Enver Akbacak[3], Melike Kaya Karaslan[1]

[1]İstanbul Provincial Health Directorate, Ministry of Health, Istanbul, Turkey
[2]Department of Electrical & Electronics Engineering, Faculty of Engineering, İstanbul University-Cerrahpaşa, İstanbul, Turkey
[3]Department of Computer Engineering, Faculty of Engineering, Beykoz University, İstanbul, Turkey

Cite this article as: N. Muzoğlu, E. Adlgüzel, E. Akbacak and M. Kaya Karaslan, "Detection of damaged structures from satellite imagery processed by autoencoder with boruta feature selection method," *Electrica*, 23(2), 397-405, 2023.

ABSTRACT

Many worldwide changing events, including meteorology, weather forecasting, disaster response, and environmental monitoring, are tracked by states or companies via satellite imagery. Early response to disasters is critical for human life. In these cases, artificial intelligence applications are also used to make rapid determinations about large geographical region. In this study, satellite images of flooded and undamaged structures in Hurricane Harvey were used. An autoencoder process has been applied to this dataset to reduce the noise in satellite imagery. AlexNet and VGG16 deep learning (DL) models are used to extract features from both datasets. The most effective features selected by the Boruta feature selection algorithm were classified with the support vector machine, and the highest classification accuracy of 99.35% was obtained. Since disasters involve the evaluation of very big datasets from large geographic areas, presenting the data with the smallest possible feature will facilitate the process. For this reason, by applying dimensionality reduction to the selected attributes, a 98.29% success was achieved in the classification with only 90 attributes. The proposed approach shows that DL and feature engineering are very effective methods to quickly respond to disaster areas using satellite imagery.
Index Terms—Autoencoder, Boruta, dimensionality reduction, transfer learning.

I. INTRODUCTION

Natural disasters have negative consequences such as property damage, loss of life, and injuries. In these cases, satellite imagery is frequently used to assess the conditions in disaster areas and provide rapid aid support. Deep learning (DL) is a software technology that can perform beyond what the human eye can detect and can be automated [1]. Convolutional DL models, which were particularly successful in the competitions held, reduced image classification error rates to less than 4% [2, 3]. Thanks to the use of artificial intelligence and DL methods, successful results have been achieved in many areas such as health care [4-8], self-driving cars [9], encryption [10], robotics [11], determining agricultural areas, cloud types, and population density from satellite images in recent years. The studies on the classification of satellite imagery using the DL approach are summarized as follows.

Unnikrishnan et al. [12] proposed the modified AlexNet model to classify wastelands, trees, large swaths, and other satellite imagery. The proposed approach reduced the number of parameters in the modified AlexNet by six times while maintaining an overall accuracy of 99.66%, which was nearly as high as that of the AlexNet. Yang et al. [13] used very high-resolution (VHR) WorldView-3 satellite images to determine the size and location of agricultural areas and achieved 99% accuracy in their classification process with fuzzy-based convolutional neural networks (CNN) models. Robinson et al. [14] used Landsat imagery with a 1-year resolution of 0.01° to estimate the U.S. population. They improved results by 4% using their proposed VGG16 approach to addressing deficiencies in survey-based censuses. Khan et al. [15] achieved a recall of 91% by using edge boxes and a CNN structure consisting of two convolutional layers, two polling layers, and 5×5 and 2×2 filters to detect military-use aircraft images from satellite imagery. Xingrui Yu et al. [16] proposed a four-layer CNN structure with shift and rotation data augmentation techniques for scene detection. They used the Sat-4 and Sat-6 datasets published by National Aeronautics and Space Administration and achieved an overall accuracy of 99.29% with their proposed approach. Patel et al. [17] used

Corresponding author:
Nedim Muzoğlu

E-mail:
nmuzoglu@gmail.com

Received: December 22, 2022

Accepted: January 11, 2023

Publication Date: March 2, 2023

DOI: 10.5152/electrica.2023.22232

different types of Yolo to detect ships using satellite imagery from the Airbus Ship Challenge and Shipsnet datasets. The highest overall accuracy was achieved with YOLOV5 at 85%. Bai et al. [18] used a combination of machine learning and feature fusion methods in their proposal. They used satellite imagery from the China National Disaster Reduction Center to compare feature differences between clouds and backgrounds and achieved an overall accuracy of 95%.

In this study, damaged and non-damaged structures were classified to detect flood-damaged structures using original satellite images and noise-free images processed in the autoencoder process. For this purpose, satellite images of flood-damaged and undamaged structures in Hurricane Harvey were used. In the proposed study, AlexNet [19] and VGG16 [20] models, which were successful in ImageNet Large Scale Visual Recognition Challenge (ILSRV) competitions, were used to extract the features of the imagery images. Since DL applications need powerful hardware, it is important to present the image with optimal attributes, especially for Big Data studies. Therefore, dimensionality reduction is applied to the subset of features selected by the Boruta algorithm. Afterward, the classification process was carried out with support vector machines (SVM), which gave successful results in many studies. As a result, the approach proposed in this study is aimed at successfully detecting flood-damaged structures with low-dimensional data.

The parts of the paper are as follows. Information about the dataset, machine learning, DL models, and the proposed approach can be found in Section II. The experimental results are described in Section III. The discussion and conclusions are described in the last section.

II. METHOD

A. Satellite Imagery Dataset

The satellite image dataset of Hurricane Harvey used in this study was obtained from open-access sources [21] and consists of two classes: damaged areas and undamaged areas. A total of 2000 images in the dataset are satellite images of 1000 damaged and 1000 undamaged structures. The size of the images of damaged and undamaged structures is 224 × 224 pixels, and the file type for all classes is jpg. The second dataset consists of reconstructed images obtained by improving the usefulness of the features by processing the dataset with the autoencoder. Sample images for the classes in the dataset are provided in Fig. 1.

B. Convolutional Neural Networks

Convolution is the process of extracting features by multiplying the input image with matrices called kernels on an element-by-element basis and summing them based on location, thus obtaining the feature maps. After obtaining feature maps, then the convolved results can be also applied with an element-wise nonlinear activation function [22] as in (1).

$$I_i^l = f\left(\sum_j I_j^{l-1} \otimes w_{ij}^l + b_i^l\right) \tag{1}$$

where I is the input patch, w is convolutional kernel for the feature value at location (i, j) for the lth layer, b is the bias, f is the activation function, and I_i^l is the feature map obtained by applying the activation function to reduce the complexity of the model and detect nonlinear features. Rectified linear unit is the most common activation function and is defined in (2).

$$f(x) = \max(0, x) \tag{2}$$

The pooling layer is typically placed between two convolutional layers. It reduces the dimensions of the activation map by preserving important features and reduces spatial invariance [22]. The pooling layer operations are defined in (3).

$$Z_k^l = g_p\left(I_{m,n,k}^l\right) \tag{3}$$

The pooling operation is applied to each feature map ($I_{:,:,k}^l$) for $\forall(m,n)$ in the local neighborhood around location (i, j), and where g_p denotes the pooling operation. The pooled feature map of lth layer for kth feature map is represented by Z_k^l [23]. The features obtained from the pooling layer are transformed into a one-dimensional vector before getting passed on to the neurons. It is called a fully connected layer because each neuron is connected to the next neuron and the layer is realized. The SoftMax function is commonly used in the final layer of CNNs to normalize the output of the fully connected layer to target class probabilities for classification tasks.

In this study, input image features are extracted from the fully connected (fc-8) layers using VGG16 and AlexNet DL models. Furthermore, the input images of the AlexNet and VGG16 models should be 227 × 227 pixels and 224 × 224 pixels, respectively. The

Fig. 1. Damaged structures after flood disaster. Undamaged structures.

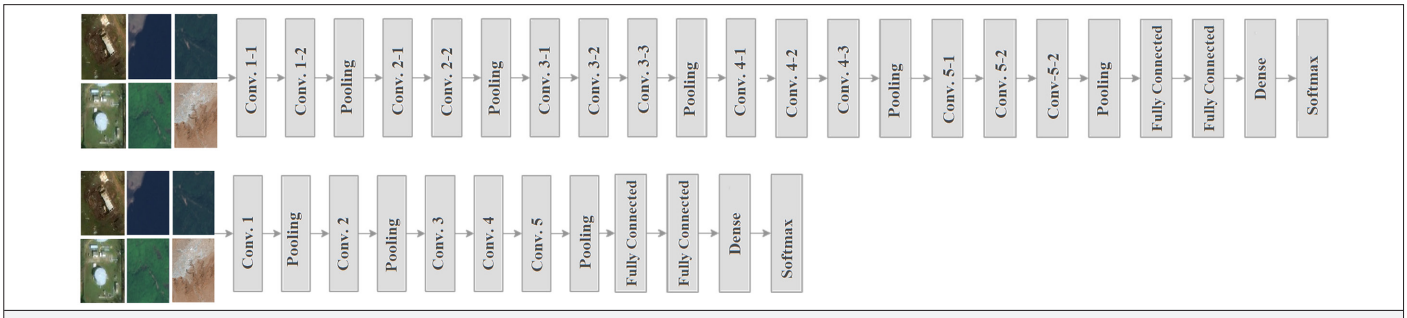

Fig. 2. The architecture of the deep convolutional neural network models. VGG16 and AlexNet.

architecture of VGG6 and AlexNet is shown in Fig. 2. The dataset was trained with fivefold cross-validation due to overfitting and lack of generalizability of a pattern.

C. Support Vector Machine

The SVM is a classification method developed to find the hyperplane that can be drawn with the largest margin between classes [24]. Support vectors are the points closest to the plane of the classes that support the plane/decision boundary as a column. The margin is the maximum width between the support vectors and the plane defined with $\frac{2}{\|w\|}$. The larger the margin between the classes, the better the separation. The hyperplane is defined by $wx+b=0$, where w is the weight vector, x is a point on the hyperplane, and b is the bias of the hyperplane from the origin. In Fig. 3, the binary classification of classes A and B with SVM is represented. In multiclass classification problems, nonlinear surfaces are linearized with the help of kernel functions, and then classification is made with support vector machines.

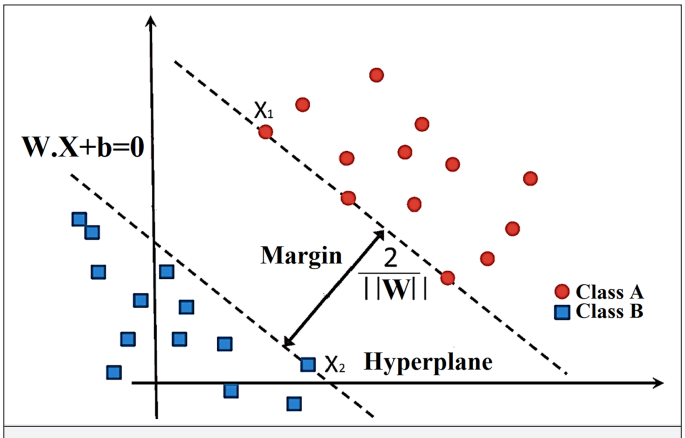

Fig. 3. Binary classification with support vector machine.

D. Feature Selection Method

Datasets are a set of features. After identifying and removing useless features from the dataset, the selected features achieve better classification success. Kursa et al. [25] proposed Boruta, which is first expanded by adding random shadow features to the original dataset and then trained by random decision forests, to distinguish important and unimportant attributes from each other. The *Z*-score is a measure of significance that is calculated by dividing the mean loss by its standard deviation. For each attribute, by calculating the *Z*-score with the highest shadow attribute, those that are too high or too low are eliminated. Variables with higher significance than random variables were considered important. Features that are of far worse importance than shadow ones are eliminated. This process continues until a specified number of iterations or until the rejection and acceptance of the features are completed [26]. In this study, Boruta feature selection algorithm based on random decision forests is used to obtain the most valuable features.

E. Autoencoder

The noise acquisition in the process of digital images with remote sensing not only degrades the visual quality but also prevents the classification and detection of the image. An autoencoder is a type of unsupervised neural network that is used to compress multidimensional data and then employs a decoder to meaningfully reconstruct data similar to that on which it has been trained in its output. In this study, autoencoders are used to reduce noise signals in satellite images. The generated noise-reduced dataset will be used to obtain useful features for feature selection [27]. The autoencoder was trained for 300 epochs and Rmsprop [28] was chosen as the optimizer. It is processed with the Keras framework using Python. Its structure and parameters are shown in Fig. 4 and Table I, respectively.

F. Principal Component Analysis

Principal component analysis (PCA) is a statistical technique used in classification and image compression to represent multidimensional data with fewer variables while preserving the high variance features [29]. For better feature engineering in datasets, it is necessary to retain features with useful information and high variance and eliminate features with highly correlated information.

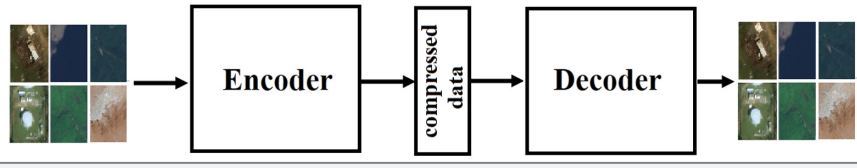

Fig. 4. The principle of the autoencoder structure.

TABLE I. AUTOENCODER MODEL SUMMARY

Layer (Type)	Output Shape	Parameters
Conv2d	128, 128, 64	1792
MaxPooling2D	64, 64, 64	0
Conv2D	64, 64, 65	18464
MaxPooling2D	32, 32, 32	0
Conv2D	32, 32, 32	4624
MaxPooling2D	16, 16, 16	0
Conv2D	16, 16, 17	2320
UpSampling2D	32, 32, 16	0
Conv2D	32, 32, 17	4640
UpSampling2D	64, 64, 32	0
Conv2D	64, 64, 64	18496
UpSampling2D	128, 128, 64	0
Conv2D	128, 128, 3	1731

Therefore, using the PCA method, variables with highly correlated features are transformed into a set of uncorrelated data in the PCA space; thus, another set of features called "principal components" is obtained. Consequently, the features in this subset should have as high a variance as possible and as low a covariance as possible. For this purpose, in the first step of PCA, the covariance matrix should be calculated to identify those features that contain redundant information. Then, the eigenvectors and eigenvalues of the covariance matrix are calculated to obtain the principal components. In Fig. 5, the features containing information in dimensions *X*1 and *X*2 are shown in the *X*2 axis after dimensionality reduction using PCA.

G. Proposed Method

In this study, a DL model is proposed to quickly detect flood-damaged structures using satellite imagery. In the first step, the satellite images are processed with an autoencoder, and the noise-reduced second feature set is obtained. Subsequently, both the 1000 features obtained from each model for each dataset and the 2000 features obtained by combining the features were classified using SVM. In the third step, a total of 4000 features extracted from the fully connected layer of the models were combined, and the most valuable subset of 200 and 400 features was determined by the Boruta feature algorithm elimination method, resulting in overall accuracy. In the next step, classification was performed using SVM by applying the PCA algorithm to reduce the dimensionality of the most valuable features. The overall block diagram of the detection model of flood-damaged structures is given in Fig. 6.

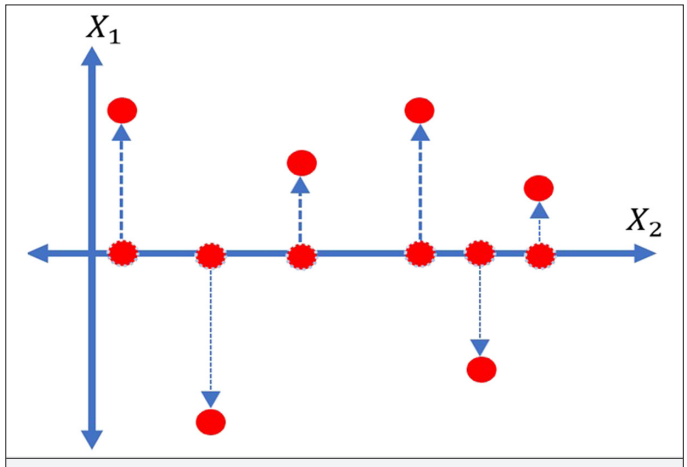

Fig. 5. The principle of the principal component analysis structure.

III. EXPERIMENTAL RESULTS

The metrics used for the evaluation of this study are sensitivity (Se), specificity (Sp), F-score (F-Scr), and accuracy (Acc). These metrics are determined by calculating the values for true positive (TP), false positive (FP), true negative (TN), and false negative (FN) from the confusion matrix using (4)–(7) below.

$$\text{Se} = \frac{TP}{TP + FN} \tag{4}$$

$$\text{Sp} = \frac{TN}{TN + FP} \tag{5}$$

$$\text{F-Scr} = \frac{2xTP}{2xTP + FP + FN} \tag{6}$$

$$\text{Acc} = \frac{TP + TN}{TP + TN + FP + FN} \tag{7}$$

In this study, the feature selection and autoencoder training were performed using the Keras framework, while the other applications were performed using Matlab 2022a. Moreover, the computer used for this study has an Nvidia GeForce RTX 3070 graphics processing unit.

In the first two steps of the study, both the 1000 features of each image extracted from the fc-8 layers of AlexNet and VGG16 and the 2000 features obtained by combining these features were classified using SVM. In detecting damaged structures using original satellite imagery, the overall accuracy values for AlexNet and VGG16 are 93% and 94.1%, respectively. Subsequently, the combined 2000 features were classified using SVM, and an overall accuracy of 94.35% was obtained. In the detection of damaged structures using autoencoder-processed satellite imagery, the overall accuracy of AlexNet and VGG16 is 94.05% and 96.05%, respectively. On the other hand, 2000 combined features from autoencoder-processed satellite images were classified using SVM, with an overall accuracy of 97.16%. The experimental results obtained in the second step are given in Fig. 7 and Table II.

In the third step, the Boruta feature selection algorithm uses a random forest to identify features in order of importance. Our experience has shown that the best success is in the range of the first 200–400 features selected in order of importance out of a total of 4000 features. The first 200 selected most valuable features were classified using SVM, and a 98.9% success was achieved, while the

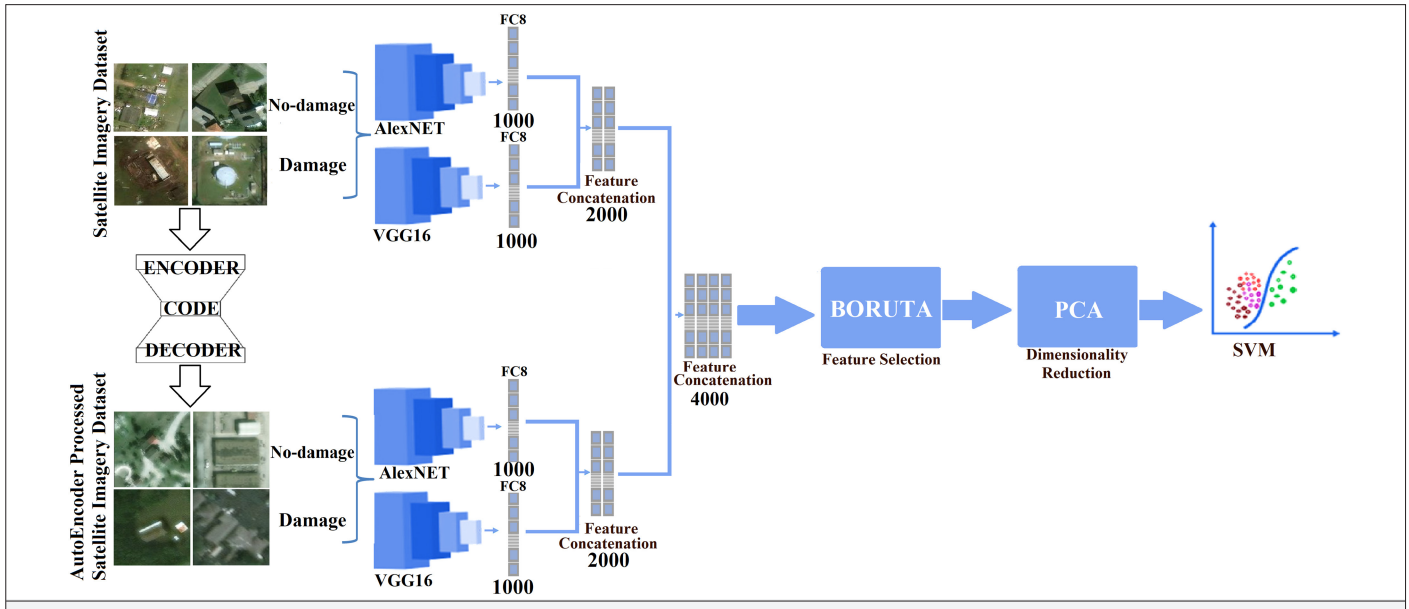

Fig. 6. The design of the proposed approach.

Fig. 7. Confusion matrix for original dataset and the autoencoder-processed dataset. AlexNet without autoencoder, VGG16 without autoencoder, AlexNet and VGG16 concatenated without autoencoder, AlexNet with autoencoder, VGG16 with autoencoder, AlexNet and VGG16 concatenated with autoencoder.

TABLE II. PERFORMANCE METRICS OBTAINED FROM THE ORIGINAL DATASET AND THE AUTOENCODER-PROCESSED DATASET

CNN Models	Feature Number	Autoencoder Model	Sensitivity (%)	Specificity (%)	F-Score (%)	Accuracy (%)
AlexNet	1000	No	92.74	93.26	93.02	93
VGG16	1000	No	95.24	92.56	93.99	94.1
AlexNet	1000	Yes	92.15	96.12	94.18	94.05
VGG16	1000	Yes	94.57	97.62	96.11	96.05
AlexNet andVGG16	2000	No	94.73	93.95	94.32	94.35
AlexNet andVGG16	2000	Yes	95.64	98.77	97.19	97.16

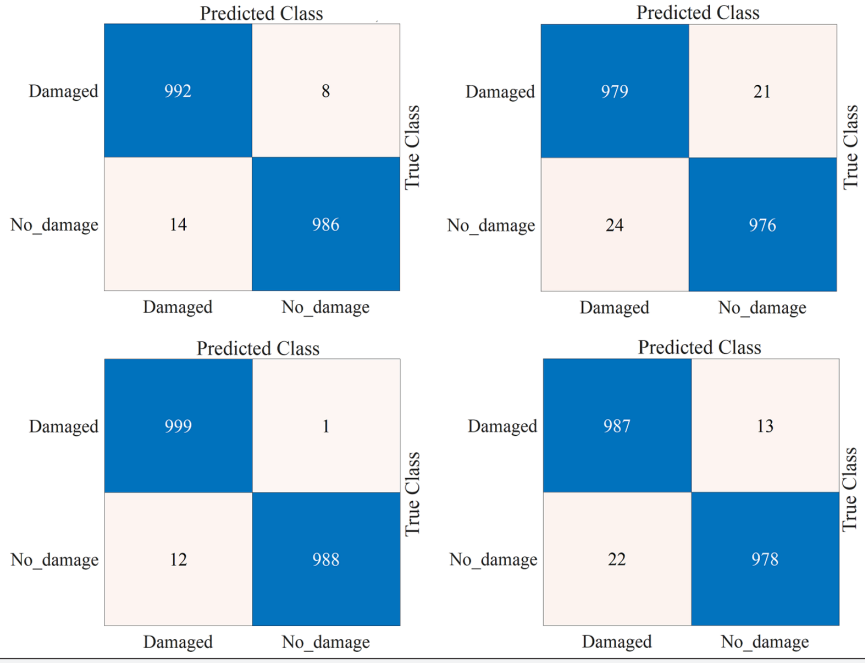

Fig. 8. Feature selection with Boruta and dimensionality reduction with principal component analysis (PCA) for concatenated features. Two hundred features selected by Boruta, 200 selected features after PCA, 400 features selected by Boruta, and 400 selected features after PCA.

overall accuracy for the 400 most valuable features was 99.35%. After that, each image represented by 200 and 400 features in the previous step was further classified by SVM after PCA processing to be represented with the least number of features possible. After dimensionality reduction, each image with 200 attributes was represented with only 61 attributes and each image with 400 attributes was represented with only 90 attributes, resulting in an overall accuracy of 97.75% and 98.29%, respectively.

The confusion matrices obtained regarding the feature selection process are given in Fig. 8. The performance metrics obtained from these matrices are given in Table III.

IV. DISCUSSION AND CONCLUSION

In this study, a DL-based flood-damaged detection system that can be used as an application in satellite systems is proposed. For this purpose, the noise encountered in satellite images was reduced by the automatic encoder process, contributing to 9.7% to the accuracy. While the original images were best classified with VGG16 with 96.05% accuracy, this value was increased by 10.3% with 2000 extracted and combined features. The highest accuracy of 99.35% was achieved using the 400 most dominant features selected by the Boruta feature selection algorithm. Since it is desired to represent the detected image with a minimum number of features, using 90 features with the applied size reduction method, classification success was achieved with 98.29% accuracy. Comparisons of the studies conducted for the flood disaster were made with the approach were recommend in Table IV.

Dotel et al. [30] used pre-disaster and post-disaster images to detect flood-damaged roads in Hurricane Harvey and preprocessed them with semantic segmentation neural networks with a differential subtraction method. The flood-damaged roads were then detected with

TABLE III. PERFORMANCE METRICS FROM FEATURE SELECTION PROCESSES WITH BORUTA

CNN Models	Selected Feature Number	Model	Feature Number After Autoencoder	Sensitivity (%)	Specificity (%)	F-Score (%)	Accuracy (%)
AlexNet and VGG16 (concatenated 4000 features)	200	Boruta	–	98.60	99.19	98.90	98.9
		Boruta and PCA	61	97.60	97.89	97.75	97.75
	400	Boruta	–	98.81	99.89	99.35	99.35
		Boruta and PCA	90	97.82	98.78	98.30	98.29

CNN, convolutional neural network; PCA, principal component analysis.

TABLE IV. COMPARISON OF THE PROPOSED MODEL WITH SIMILAR ARTICLES ON FLOOD DISASTERS

CNN Models	Model Method	Dataset	Year	Accuracy (%)
Dotel et al. [30]	Semantic segmentation U-Net, ResNet	Hurricane Harvey	2020	84.5
Cao et al. [31]	Convolutional neural networks	Hurricane Harvey	2020	97
Kaur et al. [32]	Convolutional neural networks	Hurricane Harvey	2022	97
Proposed model	Feature selection transfer learning	Hurricane Harvey	2022	99.35

84.5% accuracy in their models using the U-net and Resnet models as hybrids using the semantic segmentation method. Cao et al. [31] determined the structures damaged by flooding from Hurricane Harvey using the CNN model they developed. The model they developed has 3.5 million parameters and is smaller than the models used in the transfer learning method and detected damaged structures with 97% success. Kaur et al. [32] used the satellite imagery of Hurricane Harvey to detect structures damaged by the flood caused by the hurricane and proposed a new structure for conventional neural networks. Rmsprop achieved 97% success after 30 epochs in the study, which evaluated the results of four different optimizers.

In this study, the structures damaged by flooding in Hurricane Harvey were detected with a higher accuracy of 99.35% than in similar studies. However, the fact that the proposed approach is not an end-to-end model may have some drawbacks in its application. It is also recommended that future studies verify classification success by expanding the dataset to include various flood-damaged structures.

Peer-review: Externally peer-reviewed.

Author Contributions: Concept – N.M.; Design – N.M.; Supervision – E.Adıgüzel; Materials – E.Akbacak; Data Collection and/or Processing – E.Akbacak; Analysis and/or Interpretation – E.Adıgüzel; Literature Review - M.K.K.; Writing – N.M.;Critical Review - E.Akbacak.

Declaration of Interests: The authors have no conflicts of interest to declare.

Funding: The authors declared that this study has received no financial support.

REFERENCES

1. A. Shrestha, and A. Mahmood, "Review of deep learning algorithms and architectures," *IEEE Access*, vol. 7, pp. 53040–53065, 2019. [CrossRef]
2. M. Canayaz, "C+EffxNet: A novel hybrid approach for COVID-19 diagnosis on CT images based on CBAM and EfficientNet," *Chaos Solitons Fract.*, vol. 151, p. 111310, 2021. [CrossRef]
3. N. Muzoğlu, A. M. Halefoğlu, M. O. Avci, M. K. Karaaslan, and B. S. B. Yarman, "Detection of COVID-19 and its pulmonary stage using Bayesian hyperparameter optimization and deep feature selection methods," *Expert Syst.*, pp. e13141, 2022. [CrossRef]
4. F. ASLAN, and A. SUBAŞI, "Hemşirelik Süreci Perspektifinden yapay zeka Uygulamalarina FarkliBir Bakiş," *SBÜHD*, vol. 4, no. 3, pp. 153–158, 2022. [CrossRef]
5. A. Kaya, "'Geleceğin Teknolojisinde,' *SBÜHD sağlık bilim*," *Univ. Hemşirelik Derg.*, vol. 1, no. 3, pp. 209–214, 2019.
6. B. Akalın, and Ü. Veranyurt, "Sağlık 4.0 ve Sağlıkta yapay Zekâ," *Sağlık Profesyonelleri Araştırma Derg.*, vol. 4, no. 1, pp. 57–64, 2022.
7. İ. N. Mutlu, B. Koçak, E. Ateş Kuş, M. Baykara Ulusan, and Ö. Kılıçkesmez, "Machine learning-based computed tomography texture analysis of lytic bone lesions needing biopsy: A preliminary study," *Istanbul Med. J.*, vol. 22, no. 3, pp. 223–231, 2021. [CrossRef]
8. C. Altay *et al.*, "CT and MRI findings of orbital and paraorbital dermoid and epidermoid cyts," *Haseki Tip Bul.*, vol. 50, no. 4, pp. 127–130, 2012. [CrossRef]
9. J. Ni, Y. Chen, Y. Chen, J. Zhu, D. Ali, and W. Cao, "A survey on theories and applications for self-driving cars based on deep learning methods," *Appl. Sci.*, vol. 10, no. 8, pp. 1–29, 2020. [CrossRef]
10. Y. Zeng, H. Gu, W. Wei, and Y. Guo, "Deep-full-range: A deep learning based network encrypted traffic classification and intrusion detection framework," *IEEE Access*, vol. 7, pp. 45182–45190, 2019. [CrossRef]
11. S. Caldera, A. Rassau, and D. Chai, "Review of deep learning methods in robotic grasp detection," *Multimodal Technol. Interact.*, vol. 2, no. 3, 2018. [CrossRef]
12. A. Unnikrishnan, S. V, and S. K P, "Deep alexnet with reduced number of trainable parameters for satellite image classification," *Procedia Comput. Sci.*, vol. 143, pp. 931–938, 2018. [CrossRef]
13. R. Yang, Z. U. Ahmed, U. C. Schulthess, M. Kamal, and R. Rai, "Detecting functional field units from satellite images in smallholder farming systems using a deep learning based computer vision approach: A case study from Bangladesh," *Remote Sens. Appl. Soc. Environ.*, vol. 20, p. 100413, 2020. [CrossRef]
14. C. Robinson, F. Hohman, and B. Dilkina, "A deep learning approach for population estimation from satellite imagery," Proc. 1st ACM SIGSPATIAL Work. Geospatial Humanit. GeoHumanities, pp. 47–54, 2017. [CrossRef]
15. M. J. Khan, A. Yousaf, N. Javed, S. Nadeem, and K. Khurshid, "Automatic target detection in satellite images using deep learning," *J. SP Technol.*, vol. 7, no. 1, pp. 44–49, 2017.
16. X. Yu, X. Wu, C. Luo, and P. Ren, "Deep learning in remote sensing scene classification: A data augmentation enhanced convolutional neural network framework," *GIScience Remote Sens.*, vol. 54, no. 5, pp. 741–758, 2017. [CrossRef]
17. K. Patel, C. Bhatt, and P. L. Mazzeo, "Deep learning-based automatic detection of ships: An experimental study using satellite images," *J. Imaging*, vol. 8, no. 7, 2022. [CrossRef]
18. J. Bai *et al.*, "The epidemiological characteristics of deaths with COVID-19 in the early stage of epidemic in Wuhan, China," *Glob. Heal. Res. Policy*, vol. 5, no. 1, pp. 1–18, 2020. [CrossRef]
19. A. Krizhevsky, I. Sutskever, and G. E. Hinton, "ImageNet classification with deep convolutional neural networks [Online]." Available: http://code.google.com/p/cuda-convnet/.
20. K. Simonyan, and A. Zisserman, "Very deep convolutional networks for large-scale image recognition," 3rd Int. Conf. Learn. Represent. ICLR 2015 - Conf. Track Proc., The Hilton San Diego Resort & Spa 2015, pp. 1–14.
21. R. Al-Saffar, R. K. Mohammed, W. M. Abed, and O. F. Hussain, "Detecting Damaged Buildings on Post-Hurricane Satellite Imagery based on Transfer Learning," *NeuroQuantology*, vol. 20, no. 1, pp. 105–119, 2022. [CrossRef]
22. A. Ajit, K. Acharya, and A. Samanta, "A review of convolutional neural networks," Int. Conf. Emerg. Trends Inf. Technol. Eng. ic-ETITE 2020, 2020, pp. 1–5. [CrossRef]
23. K. Huang, A. Hussain, Q.-F. Wang, and R. Zhang, *Deep Learning: Fundamentals, Theory and Applications*, Amir Hussain, (ed.), Springer, Cham, Switzerland, 2019.
24. C. Cortes, V. Vapnik, and L. Saitta, *Support-Vector Networks Editor*. Kluwer Academic Publishers, 1995.
25. M. B. Kursa, A. Jankowski, and W. R. Rudnicki, "Boruta - A system for feature selection," *Fundam. Inform.*, vol. 101, no. 4, pp. 271–285, 2010. [CrossRef]
26. N. Muzoğlu, M. K. Karaslan, A. M. Halefoğlu, and S. Yarman, "Prediction of the prognosis of covid-19 disease using deep learning methods and Boruta Feature Selection Algorithm," *Afyon Kocatepe Univ. J. Sci. Eng.*, vol. 22, no. 3, pp. 577–587, 2022. [CrossRef]
27. M. Toğaçar, B. Ergen, and Z. Cömert, "Waste classification using AutoEncoder network with integrated feature selection method in convolutional neural network models," *Measurement*, vol. 153, 2020. [CrossRef]
28. S. Ruder, "An overview of gradient descent optimization algorithms [Online]." Available: http://arxiv.org/abs/1609.04747.

29. A. Maćkiewicz, and W. Ratajczak, "Principal components analysis (PCA)," *Comput. Geosci.*, vol. 19, no. 3, pp. 303–342, Mar. 1993. [CrossRef]
30. S. Dotel, A. Shrestha, A. Bhusal, R. Pathak, A. Shakya, and S. P. Panday, "Disaster assessment from satellite imagery by analysing topographical features using deep learning," *ACM Int. Conf. Proceeding Ser.*, pp. 86–92, 2020. [CrossRef]
31. Q. D. Cao, and Y. Choe, "Building damage annotation on post-hurricane satellite imagery based on convolutional neural networks," *Nat. Hazards*, vol. 103, no. 3, pp. 3357–3376, 2020. [CrossRef]
32. S. Kaur, S. Gupta, S. Singh, D. Koundal, and A. Zaguia, "Convolutional neural network based hurricane damage detection using satellite images," *Soft Comput.*, vol. 26, no. 16, pp. 7831–7845, 2022. [CrossRef]

Nedim Muzoğlu completed his master's degree in Biomedical, Electronic Engineering and completed PhD degree in Biomedical Engineering. He studied artificial intelligence, deep learning, diagnostic radiology, and clinical engineering during his studies. In 2002/2010, he worked in the IT departments in the field of telecommunications. He has been working as a Clinical Engineering Department Manager in Public Hospitals Institutions since 2010.

Ertuğrul Adigüzel completed his undergraduate degree and MSc degrees in Electrical Engineering. He has studied in the field of Renewable Energy Resources during his MSc. He has been working as a Research Assistant in İstanbul University-Cerrahpasa since 2018.

Enver Akbacak completed his MSc and PhD degree in Electrical Engineering. He has studied in the field of image processing and artificial intelligence during his PhD. He has been working as an IT Engineer in Public Hospitals Institutions since 2009 and manages the information systems of health service providers.

Melike Kaya Karaaslan received her undergraduate degree in Physics Engineering from the University of Ankara, Turkey, in 2004, and her MSc in Biomedical Engineering from the University of Kocaeli. She continues her PhD at Kocaeli University. Her research focuses on the diagnostic radiology, medical physics, and artificial intelligence. She has been working as a Physics Engineer in Public Hospitals Institutions since 2013 and carries out quality control and acceptance tests of diagnostic radiology devices.